Supplementary Information

S1 Observational analysis: methodology

Derivation of the canopy resistance from the observation-derived deposition velocity requires knowledge on the aerodynamic resistance (r_a) and the quasi-laminar layer resistance (r_b). Above-canopy aerodynamic resistance is calculated as follows:

$$r_a = \frac{\ln\left(\frac{z_r - d}{z_{0m}}\right) - \Psi(\frac{z_r - d}{L})}{k u_*}$$

with k the Von Kármán constant (0.40) [unitless], u_* is friction velocity [m s^{-1}], z_r is the reference height (set to the canopy height), z_{0m} is the roughness length for momentum (set at a typical value for forests of 1.1 m), and d the displacement height (set to 2/3 of the canopy height). L is the Obukhov Length, calculated as follows:

$$L = \frac{-u_*^3}{kg\frac{H}{T_v c_p \rho_a}}$$

With g the gravitational acceleration [9.81 m s^{-2}], H is the sensible heat flux [W m^{-2}], T_v is the virtual temperature [K], c_p the specific heat capacity of air [1010 J K^{-1} kg^{-1}], and ρ_a the air density at 298K and 1013 hPa [1.225 kg m^{-3}]. Ψ is the stability correction function reflecting Monin-Obukhov Similarity Theory (Foken, 2006), as applied in Clifton et al. (2017):

$$\Psi = \begin{cases} 2ln\left(\frac{1 + \left(0.95\left(1 - 11.6\frac{z_r - d}{L}\right)^{\frac{1}{2}}\right)}{2}\right) & if\ -2 \leq \frac{z_r - d}{L} < 0 \\ -7.8\frac{z_r - d}{L} & if\ 0 \leq \frac{z_r - d}{L} < 1 \end{cases}$$

r_b is the quasi-laminar layer resistance, calculated following Wesely and Hicks (1977):

$$r_b = \frac{2}{k u_*}\left(\frac{\kappa}{D_{O_3}}\right)^{2/3}$$

With κ being the thermal diffusivity of air [0.2 cm^2 s^{-1}], and D_{O_3} the diffusivity of ozone [0.13 cm^2 s^{-1}] (Wesely 1989).

S2 Dependence of non-stomatal deposition on driving variables: MLC-CHEM sensitivity experiments

With a range of MLC-CHEM sensitivity experiments (See Table S1), we aim to further understand the observed temperature and VPD sensitivity of the non-stomatal ozone removal fraction ($g_{ns}g_c^{-1}$). With this analysis, we aim to assess the role of each process in explaining temporal variability in non-stomatal ozone removal. We focus this sensitivity analysis on the Ispra observations and simulations, since the non-stomatal ozone sink for Hyytiälä has been characterized before (Rannik et al. 2012), but we display the temperature and VPD sensitivity of $g_{ns}g_c^{-1}$ for Hyytiälä in Figures S4 and S5.

Figure S4 displays the MLC-CHEM-simulated temperature sensitivity of non-stomatal ozone removal after deactivating various non-stomatal removal processes. Deactivated wet leaf deposition (NWL) reduces $g_{ns}g_c^{-1}$ under low-temperature conditions by up to 21%, particularly during the morning when humid conditions prevail (Fig. S4b). This effect is even more pronounced under low-humidity conditions, when $g_{ns}g_c^{-1}$ is reduced by more than 0.2 during the morning (Fig. S4e). Deactivated soil uptake (NSL) most strongly reduces the non-stomatal fraction during high-temperature conditions in the afternoon, by up to 38% (Fig. S4d). This reflects increasing atmospheric instability with temperature in MLC-CHEM, that results in simulated increases in turbulent transport in the canopy (Fig. S3). To further evaluate the sensitivity of the simulated non-stomatal ozone removal fraction to turbulent transport in the understory, we conducted an additional experiment in which the eddy diffusivity for transport between the crown layer and the understory layer was strongly enhanced (NTG). Contrary to our expectations, this experiment leads to a decreased non-stomatal fraction by 2-10%. This reflects enhanced stomatal uptake in the understory, which is more efficient than soil deposition. Deactivating temperature-dependent removal (NCH) leads to little change (<2%) in the non-stomatal ozone removal fraction.

Table S1. Setup of MLC-CHEM sensitivity experiments in Section 3.3, and hypotheses regarding the change in the non-stomatal ozone removal fraction ($g_{ns}g_c^{-1}$).

Experiment name	**Code modification**	**Hypothesized effect on T_a/VPD sensitivity**
DEF (Default)	MLC-CHEM setup as in paper	-
NWL (no wet leaf uptake)	$f_{ws} = 0$	Reduced $g_{ns}g_c^{-1}$under high-humidity conditions
NSL (no soil deposition)	$r_{soil} = 10^5$ s m^{-1}	Reduced $g_{ns}g_c^{-1}$under high-temperature conditions
NCH (no in-canopy chemistry)	Chemical reactions turned off	Reduced $g_{ns}g_c^{-1}$under high-temperature conditions
NTG (no vertical turbulence gradient)	Lower-canopy eddy diffusivity set to upper-canopy eddy diffusivity	Increased $g_{ns}g_c^{-1}$due to more efficient transport to the soil

S3 Supplementary Figures

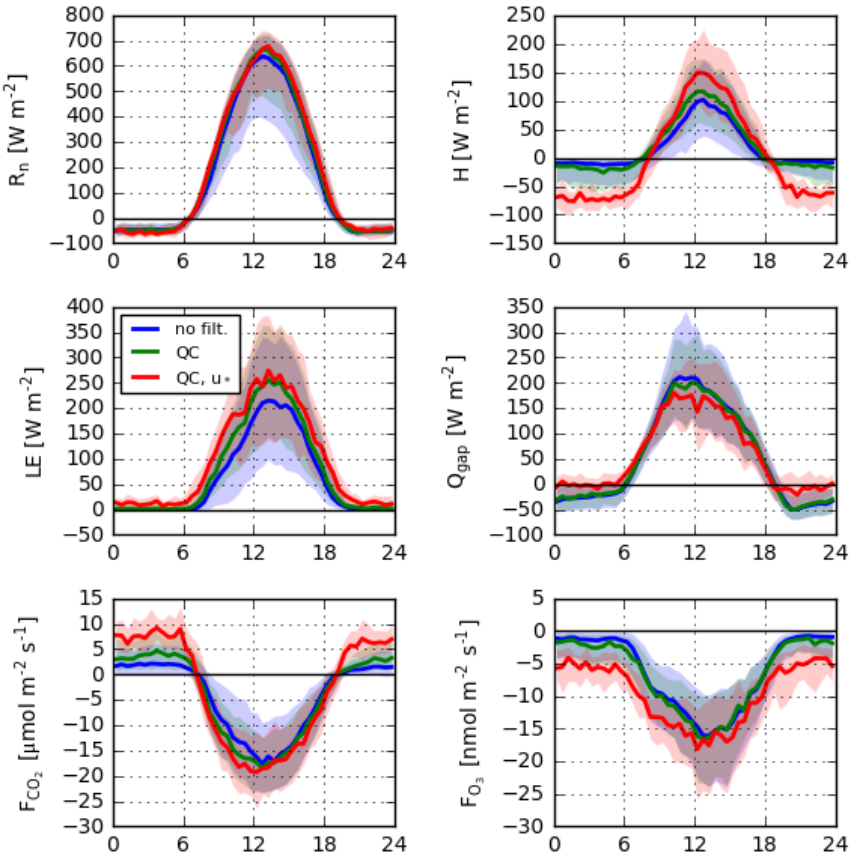

Figure S1. Median April-September 2013-2015 diurnal cycles of net radiation, sensible and latent heat fluxes, surface energy balance closure gap, CO2 flux and ozone flux before and after gap correction. Blue lines depict unfiltered data, green lines show the data after quality-control (QC) filtering (discarding poor quality flux observations), and red lines show QC- and u*-filtered data (based on a u* threshold of 0.35 m s^{-1}, determined using the REddyProcWeb tool (Wutzler et al. 2018).

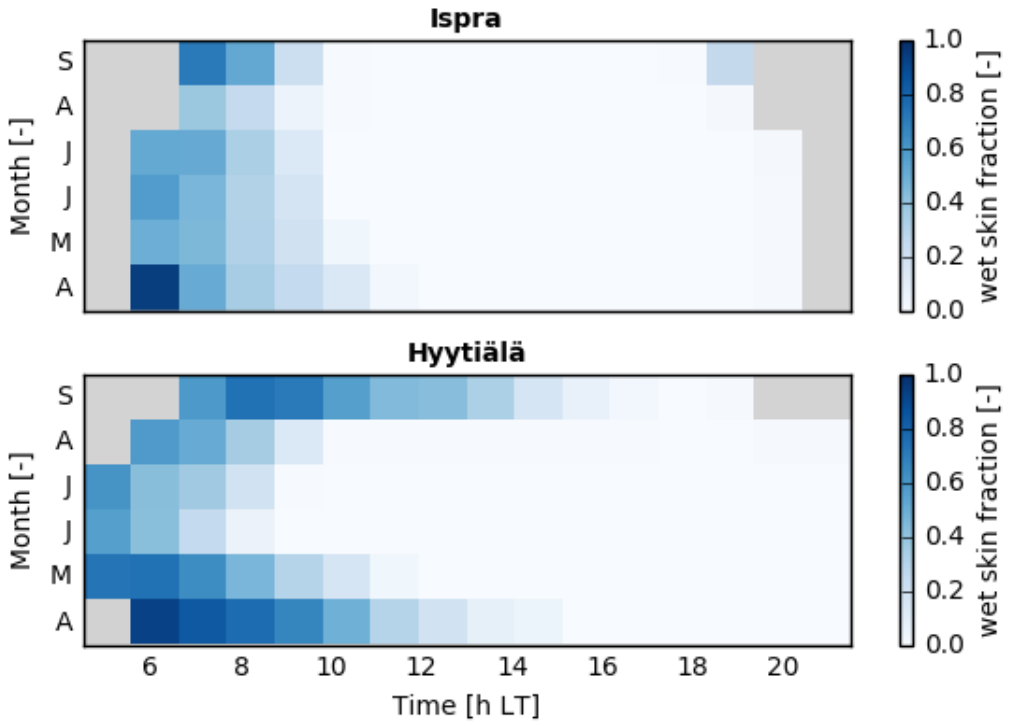

Figure S2. Mean values of the MLC-CHEM canopy wet skin fraction binned by month and hour for Ispra (2013-2015) and Hyytiälä (2002-2011) during April-September.

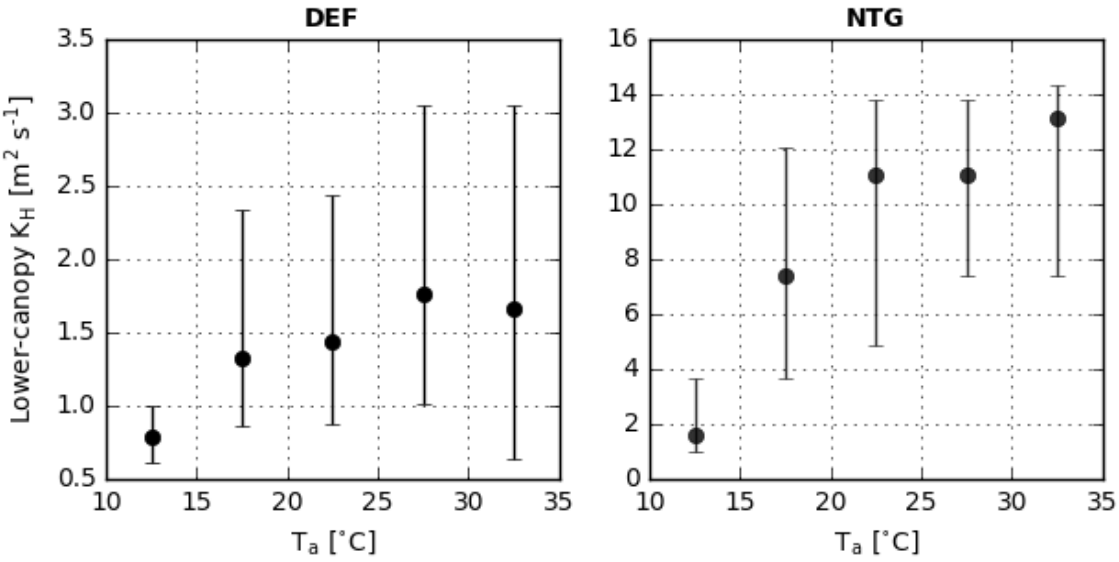

Figure S3. Lower-canopy eddy diffusivity (K_H) binned by air temperature (in steps of $5°C$ for the default simulation for Ispra in the default MLC-CHEM simulation (DEF) and the simulation with a deactivated gradient in turbulent mixing (NTG).

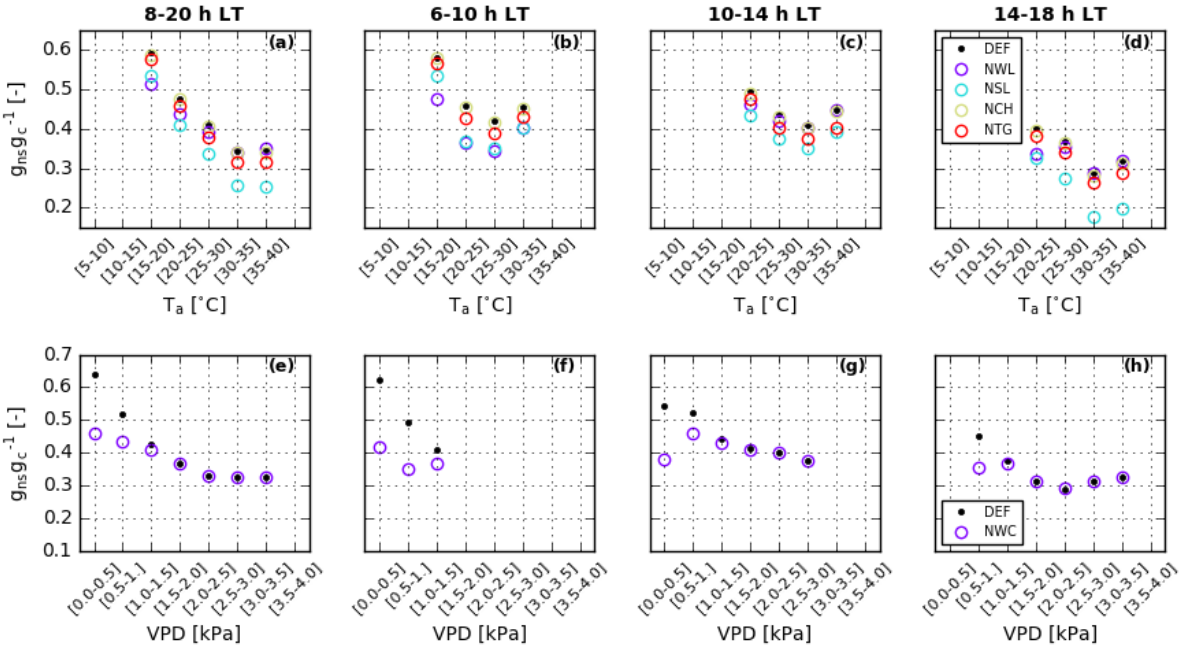

Figure S4. Non-stomatal ozone removal fraction ($g_{ns}g_c^{-1}$) binned by air temperature (panels a-d) and vapour pressure deficit (panels e-h) in the MLC-CHEM sensitivity experiments for Ispra (see Table S1 for experiment abbreviations).

References

Clifton, O.E., Fiore, A.M., Munger, J.W., Malyshev, S., Horowitz, L.W., Shevliakova, E., Paulot, F., Murray, L.T., Griffin, K.L. (2017). Interannual variability in ozone removal by a temperature deciduous forest. Geophysical Research Letters, 44, p. 542-552, https://doi.org/10.1002/2016GL070923.

Foken, T. (2006). 50 years of the Monin-Obukhov similarity theory, Boundary Layer Meteorology, 119, 431-447, https://doi.org/10.1007/s10546-006-9048-6.

Rannik, Ü., Altimir, N., Mammarella, I., Bäck, J., Rinne, J., Ruuskanen, T.M., Hari, P., Vesala, T., Kulmala, M. (2012). Ozone deposition into a boreal forest over a decade of observations: evaluating deposition partitioning and driving variables. Atmospheric Chemistry and Physics, 12, p. 12165-12182, https://doi.org/10.5194/acp-12-12165-2012.

Wesely, M.L., Hicks, B.B. (1977). Some factors that affect the deposition rates of sulfur dioxide and similar gases on vegetation. Journal of the Air Pollution Control Association, 27(11), 1110-1116, https://doi.org.10.1080/00022470.1977.10470534.

Wesely, M.L. (1989). Parameterization of surface resistances to gaseous dry deposition in regional-scale numerical models. Atmospheric Environment, 23, p. 1293-1304, https://doi.org.10.1016/j.atmosenv.2007.10.058.

Wutzler, T., Lucas-Moffat, A., Migliavacca, M., Knauer, J., Sickel, K., Sigut, M.O, Reichstein, M. (2018). Basic and extensible post-processing of eddy covariance flux data with REddyProc. Biogeosiences, 15, p. 5015-5030, https://doi.org/10.5194/bg-15-5015-2018.